COMPRESSIVE WIDE-BAND SPECTRUM SENSING

Yvan Lamelas Polo[⋆†] *Ying Wang*[†] *Ashish Pandharipande*[†] *Geert Leus*[⋆]

[⋆]Faculty of Electrical Engineering, Delft University of Technology, The Netherlands
[†]Philips Research Europe, Eindhoven, The Netherlands
Email: {yvan.lamelas.polo, ying.z.wang, ashish.p}@philips.com, g.j.t.leus@tudelft.nl

ABSTRACT

We present a compressive wide-band spectrum sensing scheme for cognitive radios. The received analog signal at the cognitive radio sensing receiver is transformed in to a digital signal using an analog-to-information converter. The autocorrelation of this compressed signal is then used to reconstruct an estimate of the signal spectrum. We evaluate the performance of this scheme in terms of the mean squared error of the power spectrum density estimate and the probability of detecting signal occupancy.

***Index Terms*—** Compressive sampling, Wide-band spectrum sensing, Cognitive radio, Spectrum estimation.

1. INTRODUCTION

It has been widely recognized that utilization of radio spectrum by licensed wireless systems, e.g., TV broadcasting, aeronautical telemetry, is quite low [6]. In particular, at any given time and spatial region, there are frequency bands where there is no signal occupancy. That is, licensed signal transmissions are sparse in frequency domain. There has been recent interest in improving spectrum utilization by permitting secondary usage using cognitive radios [1], [6], [12]. Cognitive radios use spectrum sensing to determine frequency bands that are vacant of licensed signal transmissions and transmit on such portions to meet regulatory constraints of avoiding harmful interference to licensed systems.

Future cognitive radios will be capable of scanning a wide band of frequencies [1], in the order of a few GHz, and employ adaptive waveforms for transmission depending on the estimated spectrum of licensed systems. In this paper, we address the problem of estimating the spectrum of the wide-band signal received at the cognitive radio sensing receiver using compressive sampling.

Compressive sampling (CS) is a method for acquisition of sparse signals at rates significantly lower than Nyquist rate; signal reconstruction is a solution to an optimization problem [2], [5]. In [11], a spectrum sensing scheme based on compressive sampling was introduced which works for special signals whose fourier transform is real. For the scheme in [11] to work for a larger class of signals, we first consider the following extension. The signal received from the licensed system at the cognitive radio sensing receiver is sampled, albeit at the Nyquist rate. The autocorrelation of the resulting signal is compressively sampled. An estimate of the spectrum is then obtained using a wavelet edge detector after CS reconstruction, thus determining the spectrum occupancy of the licensed system. This scheme still requires an analog-to-digital converter (ADC) to operate at Nyquist rate or higher and takes a paradoxical approach to CS. Wide-band ADCs operating at sampling rates of the order of several giga-samples/s are thus a major challenge with such a scheme.

We consider a spectrum sensing scheme based on compressive sampling of the wide-band analog signal using an analog-to-information converter (AIC). An AIC directly relates to the idea of sampling at the information rate of the signal. Practical approaches to AIC design have been considered in [8], [10]. An estimate of the original signal spectrum is then made based on CS reconstruction using a wavelet edge detector along the approach in [11]. We evaluate the resulting power spectrum density (PSD) estimate using the mean squared error (MSE) and the probability of detecting spectrum occupancy, and compare the performance with the scheme based on [11]. We note that for the scheme based on [11], CS is done on the autocorrelation of the discrete-time signal obtained by Nyquist-rate sampling. In our approach, CS is directly performed on the wide-band analog signal.

2. PRELIMINARIES

Let $x(t)$ be the wide-band analog signal received at the cognitive radio sensing receiver. We consider the frequency range of interest to be comprised of P non-overlapping contiguous subbands. The bandwidth and channelization of the subbands need not in general be known to the cognitive radio.

We shall first follow [2], [5] and [11] to describe a scheme for wide-band spectrum sensing based on CS principles. Let the analog signal $x(t)$, $0 \leq t \leq T$, be represented as a finite weighted sum of basis functions (e.g., Fourier) $\psi_i(t)$ as follows

$$x(t) = \sum_{i=1}^{N} s_i \psi_i(t) \tag{1}$$

where only a few basis coefficients s_i are much larger than zero due to the sparsity of $x(t)$. In particular, with a discrete-time CS framework, consider the acquisition of an $N \times 1$ vector $\mathbf{x} = \mathbf{\Psi s}$, where $\mathbf{\Psi}$ is the $N \times N$ sparsity basis matrix and $\mathbf{s}$ an $N \times 1$ vector with $K \ll N$ non-zero (and large enough) entries s_i. It has been shown that $\mathbf{x}$ can be recovered using $M = K\mathcal{O}(\log N)$ non-adaptive linear projection measurements on to an $M \times N$ basis matrix $\mathbf{\Phi}$ that is incoherent with $\mathbf{\Psi}$ [3]. An example construction of $\mathbf{\Phi}$ is by choosing elements that are drawn independently from a random distribution, e.g., Gaussian, Bernoulli. The measurement vector $\mathbf{y}$ can be written as

$$\mathbf{y} = \mathbf{\Phi x} = \mathbf{\Phi \Psi s}. \tag{2}$$

Reconstruction is achieved by solving the following l_1-norm optimization problem

$$\hat{\mathbf{s}} = \arg\min_{\mathbf{s}} \|\mathbf{s}\|_1 \quad \text{s.t.} \quad \mathbf{y} = \mathbf{\Phi \Psi s}. \tag{3}$$

Linear programming techniques, e.g., basis pursuit [4], or iterative greedy algorithms [9] can be used to solve (3).

2.1. Compressive spectrum sensing scheme based on [11]

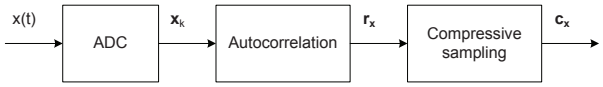

Fig. 1. CS acquisition in spectrum sensing method of [11].

The compressive spectrum sensing approach presented in [11] works under the assumption that the frequency response of the analog signal input at the sensing receiver is real, with a relatively flat response over its regions of support. To make the method of [11] to work in practice, we consider the following simple extension. Figure 1 depicts the CS acquisition employed. The basic idea of this approach is to view the entire wide-band spectrum as subbands where subband edges indicate change in spectrum occupancy. These spectrum edges can be detected using a wavelet-based detector. The CS method is applied to wide-band spectrum sensing as follows. The received signal $x(t)$ is sampled at Nyquist rate or higher and the discrete-time signal stacked in to $N \times 1$ vectors

$$\mathbf{x}_k = [x_{kN} \;\; x_{kN+1} \;\cdots\; x_{kN+N-1}]^T, \quad k = 0, 1, 2, \ldots \tag{4}$$

where ^{T} denotes the transpose operation. We assume the signal to be zero-mean, wide-sense stationary. Denote the autocorrelation at lag j as $r_x(j) = E[x_n x^*_{n-j}]$. In practice, estimates of the autocorrelation are obtained by averaging over several signal segments. Denote the $2N \times 1$ autocorrelation vector of (4) as

$$\mathbf{r_x} = [0 \; r_x(-N+1) \;\cdots\; r_x(0) \;\cdots\; r_x(N-1)]^T. \tag{5}$$

A wavelet-based smoothing is then performed, followed by taking a Fourier transform to obtain the PSD. Denote the discrete counterparts of these operations by the $2N \times 2N$ matrices $\mathcal{W}$ and $\mathcal{F}$. The derivative of the PSD then gives the edge spectrum. The derivative can be approximated by a first-order difference, given by the $2N \times 2N$ matrix

$$\mathbf{\Gamma} = \begin{bmatrix} 1 & 0 & \cdots & 0 \\ -1 & 1 & \cdots & 0 \\ & \ddots & \ddots & \vdots \\ 0 & \cdots & -1 & 1 \end{bmatrix}.$$

Denote $\mathbf{G} = (\mathbf{\Gamma}\mathcal{F}\mathcal{W})^{-1}$. Note that $\mathbf{G}$ represents the transform domain where the autocorrelation vector $\mathbf{r_x}$ has a sparse representation. The $2N \times 1$ discrete component vector $\mathbf{z_s}$ corresponding to the edge spectrum can be related to $\mathbf{r_x}$ by [11]

$$\mathbf{r_x} = \mathbf{G}\mathbf{z_s} \tag{6}$$

Compressive sampling is now performed by means of a $2M \times 2N$ compressive matrix $\mathbf{\Phi}_I$, giving rise to the $2M \times 1$ measurement vector $\mathbf{c_x} = \mathbf{\Phi}_I \mathbf{r_x}$. An estimate $\hat{\mathbf{z}}_{\mathbf{s},1}$ of the edge spectrum is obtained by solving the CS reconstruction problem:

$$\hat{\mathbf{z}}_{\mathbf{s},1} = \arg\min_{\mathbf{z_s}} \|\mathbf{z_s}\|_1 \quad \text{s.t.} \quad \mathbf{c_x} = (\mathbf{\Phi_I G})\mathbf{z_s}. \tag{7}$$

An estimate of the wide-band spectrum can be obtained from $\hat{\mathbf{z}}_{\mathbf{s},1} = [\hat{z}_{\mathbf{s},1}(1) \; \hat{z}_{\mathbf{s},1}(2) \;\cdots\; \hat{z}_{\mathbf{s},1}(2N)]^T$ by computing a cumulative sum. The discrete components of the PSD estimate are given by

$$\hat{S}_{\mathbf{x},1}(n) = \sum_{k=1}^{n} \hat{z}_{\mathbf{s},1}(k). \tag{8}$$

It is important to point out that this scheme results in a somewhat paradoxical architecture since sub-Nyquist sampling is achieved by first sampling the wide-band analog signal at Nyquist rate and then applying CS on the autocorrelation vector $\mathbf{r_x}$.

3. COMPRESSIVE SPECTRUM SENSING WITH AIC

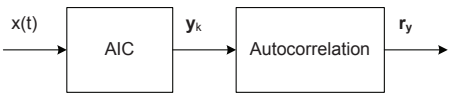

Fig. 2. CS acquisition in proposed spectrum sensing method.

Figure 2 depicts the acquisition under the proposed method. The analog baseband signal $x(t)$ is sampled using an AIC. An AIC may be conceptually viewed as an ADC operating at Nyquist rate, followed by compressive sampling. Denote the $N \times 1$ stacked vector at the output of the ADC by

$$\mathbf{x}_k = [x_{kN} \;\; x_{kN+1} \;\cdots\; x_{kN+N-1}]^T \quad k = 0, 1, 2 \ldots \tag{9}$$

and the $M \times N$ compressive sampling matrix by $\mathbf{\Phi}_A$. The output of the AIC denoted by the $M \times 1$ vector

$$\mathbf{y}_k = [y_{kM} \;\; y_{kM+1} \;\cdots\; y_{kM+M-1}]^T \quad k = 0, 1, 2 \ldots \tag{10}$$

is given by

$$\mathbf{y}_k = \mathbf{\Phi}_A \mathbf{x}_k. \tag{11}$$

The respective $N \times N$ and $M \times M$ autocorrelation matrices of the compressed signal and the input signal vectors in (10) and (9) are related as follows

$$\mathbf{R_y} = E[\mathbf{y}_k \mathbf{y}_k^H] = \mathbf{\Phi}_A \mathbf{R_x} \mathbf{\Phi}_A^H \tag{12}$$

where ^{H} denotes the Hermitian. The elements of the matrices in (12) are given by: $[\mathbf{R_y}]_{ij} = r_y(i-j) = r_y^*(j-i)$, $[\mathbf{R_x}]_{ij} = r_x(i-j) = r_x^*(j-i)$.

Denote the respective $2N \times 1$ and $2M \times 1$ autocorrelation vectors corresponding to (9) and (10) as follows

$$\mathbf{r_x} = [0 \;\; r_x(-N+1) \;\cdots\; r_x(0) \;\cdots\; r_x(N-1)]^T, \tag{13}$$

$$\mathbf{r_y} = [0 \;\; r_y(-M+1) \;\cdots\; r_y(0) \;\cdots\; r_y(M-1)]^T. \tag{14}$$

To pose the CS reconstruction in the form of (3) and (7), we need to first relate the autocorrelation vectors in (13) and (14). Note that the components of these vectors lie on the first column and row of the respective autocorrelation matrices. After some matrix algebraic operations, we obtain the following result.

$$\mathbf{r_y} = \mathbf{\Phi}_{II} \mathbf{r_x} \tag{15}$$

where $\mathbf{\Phi}_{II}$ is given as

$$\mathbf{\Phi}_{II} = \begin{bmatrix} \overline{\mathbf{\Phi}}_A \mathbf{\Phi}_1 & \overline{\mathbf{\Phi}}_A \mathbf{\Phi}_2 \\ \mathbf{\Phi}_A \mathbf{\Phi}_3 & \mathbf{\Phi}_A \mathbf{\Phi}_4 \end{bmatrix}. \tag{16}$$

Denoting the (i,j)-th element of $\mathbf{\Phi}_A$ by $\phi^*_{i,j}$, the $M \times N$ matrix $\overline{\mathbf{\Phi}}_A$ has its (i,j)-th element given by

$$[\overline{\mathbf{\Phi}}_A]_{i,j} = \begin{cases} 0 & i = 1, \; j = 1, \cdots, N, \\ \phi_{M+2-i,j} & i \neq 1, \; j = 1, \cdots, N, \end{cases}$$

and the $N \times N$ matrices $\mathbf{\Phi}_1, \mathbf{\Phi}_2, \mathbf{\Phi}_3, \mathbf{\Phi}_4$ are

$$\mathbf{\Phi}_1 = hankel([\mathbf{0}_{N\times 1}], [0 \;\; \phi^*_{1,1} \;\cdots\; \phi^*_{1,N-1}])$$

$$\mathbf{\Phi}_2 = hankel([\phi^*_{1,1} \;\cdots\; \phi^*_{1,N}], [\phi^*_{1,N} \;\; \mathbf{0}_{1\times(N-1)}])$$

$$\mathbf{\Phi}_3 = toeplitz([\mathbf{0}_{N\times 1}], [0 \;\; \phi_{1,N} \;\cdots\; \phi_{1,2}])$$

$$\mathbf{\Phi}_4 = toeplitz([\phi_{1,1} \;\cdots\; \phi_{1,N}], [\phi_{1,1} \;\; \mathbf{0}_{1\times(N-1)}]),$$

where $hankel(\mathbf{c}, \mathbf{r})$ is a hankel matrix (i.e., symmetric and constant across the anti-diagonals) whose first column is $\mathbf{c}$ and whose last row is $\mathbf{r}$, $toeplitz(\mathbf{c}, \mathbf{r})$ is a toeplitz matrix (i.e., symmetric and constant across the diagonals) whose first column is $\mathbf{c}$ and whose first row is $\mathbf{r}$, $\mathbf{0}_{N\times 1}$ is a column of N zeros, and $\mathbf{0}_{1\times(N-1)}$ is a row of $N-1$ zeros.

Now using (6) and (15), we can formulate the CS reconstruction of the edge spectrum as an l_1-norm optimization problem

$$\hat{\mathbf{z}}_{\mathbf{s},2} = \arg\min_{\mathbf{z_s}} \|\mathbf{z_s}\|_1 \quad \text{s.t.} \quad \mathbf{r_y} = (\mathbf{\Phi}_{II}\mathbf{G})\mathbf{z_s} \tag{17}$$

An estimate of the wide-band spectrum can now be obtained, as done in Section 2.1, from $\hat{\mathbf{z}}_{\mathbf{s},2} = [\hat{z}_{\mathbf{s},2}(1)\ \hat{z}_{\mathbf{s},2}(2)\ \cdots\ \hat{z}_{\mathbf{s},2}(2N)]^T$ by computing a cumulative sum. The discrete components of the PSD estimate are given by

$$\hat{S}_{\mathbf{x},2}(n) = \sum_{k=1}^{n} \hat{z}_{\mathbf{s},2}(k). \tag{18}$$

In [3], the mutual coherence parameter μ is defined as a measure of the incoherence between the compressive sampling matrix $\mathbf{\Phi}$ and sparsity basis matrix $\mathbf{\Psi}$ involved in CS,

$$\mu(\mathbf{\Phi}, \mathbf{\Psi}) = \sqrt{2N} \cdot \max_{1\le k\le 2M, 1\le j\le 2N} |\langle \phi_k, \psi_j \rangle|, \tag{19}$$

$$\mu(\mathbf{\Phi}, \mathbf{\Psi}) \in [1, \sqrt{2N}]$$

where ϕ_k and ψ_j are respective columns of $\mathbf{\Phi}$ and $\mathbf{\Psi}$. The proposed scheme incurs a reduced mutual incoherency due to the structure of $\mathbf{\Phi}_{II}$ in (16). This has an impact on the performance of spectrum estimation and subsequent detection, as will be shown via simulation results.

4. SIMULATION RESULTS

In this section we evaluate the performance of the proposed AIC-based spectrum sensing scheme (Architecture II) with that presented in Section 2.1 (Architecture I). We consider, at baseband, a wide frequency band of interest ranging from -40 to 40 MHz, containing 10 non-overlapping channels of equal bandwidth of 8 MHz. Each channel is possibly occupied by a licensed system transmission signal that uses OFDM modulation according to the DVB-T standard. Each 8 MHz OFDM symbol has 8192 frequency tones and a cyclic prefix length of 1024. The number of OFDM symbols used for spectrum sensing is 1. The over-sampling factor is 16, i.e. the sampling rate is 16×8MHz. The occupancy ratio of the total 80 MHz band is 50%, i.e., 5 out of 10 channels are occupied by licensed transmission signals and the remaining 5 channels are unoccupied. The received signal is corrupted by additive white Gaussian noise (AWGN) with a variance of $\sigma_n^2 = 0.2$. The received signal to noise ratios (SNR) of the 5 active channels are 7dB, 4dB, 7dB, 7dB, and 4dB, respectively. A Gaussian wavelet function is used for smoothing. For compressed sensing, N is 256 and the compression rate M/N is set to vary from 1% to 100%. The entries of the compressive sampling matrix $\mathbf{\Phi}$ are Gaussian distributed with zero mean and variance $1/M$.

The estimated / recovered PSD: Figure 3 shows the estimated PSD based on our proposed approach. The top plot shows the original PSD of the received wide-band signal. The middle plot shows the estimated edge vector $\hat{\mathbf{z}}_{\mathbf{s},2}$ in (17) using a tree-based Matching Pursuit recovery from the CS measurements with M/N=0.5. The bottom plot shows the recovered PSD $\hat{\mathbf{S}}_{\mathbf{x},2}$ vectors whose elements are defined as in (18) via cumulative sum of the estimated edge vector.

MSE performance: We compare the normalized MSE of the estimated PSD of our approach and that of [11]. The normalized MSE is defined as

$$\text{MSE}_i = E\{\frac{\|\hat{\mathbf{S}}_{\mathbf{x},i} - \mathbf{S}_{\mathbf{x}}\|_2^2}{\|\mathbf{S}_{\mathbf{x}}\|_2^2}\}, \quad i = 1, 2 \tag{20}$$

where $\mathbf{S}_{\mathbf{x}}$ denotes the PSD estimate vector based on the periodogram using the signals sampled at Nyquist rate, $\hat{\mathbf{S}}_{\mathbf{x},1}$ the PSD estimate vector based on the approach of [11], and $\hat{\mathbf{S}}_{\mathbf{x},2}$ the PSD estimate vector based on our approach. We can see from figure 4 that for both approaches the signal recovery quality (via tree-based Matching Pursuit) improves as the compression rate M/N increases. While the MSE performance of our approach is a bit worse than that of the method described in Section 2.1 due to the reduced mutual incoherency of $\mathbf{\Phi}_{II}$ in (16), a reduced sampling rate is employed in our approach.

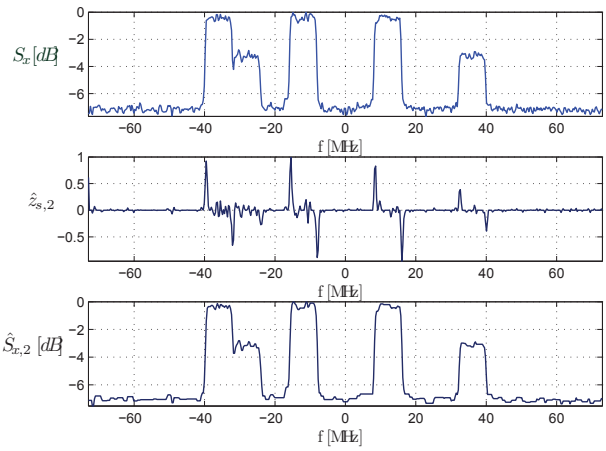

Fig. 3. Spectrum estimation: (a) Nyquist rate PSD; (b) recovered edge spectrum; (c) recovered PSD from edges

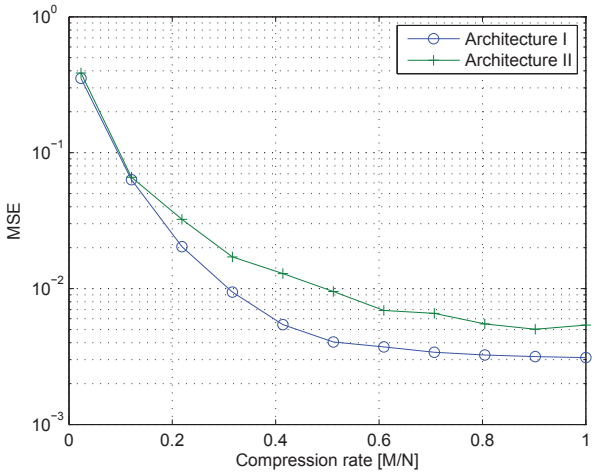

Fig. 4. MSE performance

Probability of Detection Performance: We evaluate the probability of detection P_d based on the estimated PSD $\hat{\mathbf{S}}_{\mathbf{x},i}, i = 1, 2$. The decision of the presence of a licensed transmission signal in a certain channel is made by an energy detector using the estimated frequency response over that channel, i.e., the test statistic is

$$T_p = \sum_{k=(p-1)K+1}^{pK} \hat{S}_{\mathbf{x},i}(k), \quad p = 1, 2, \ldots, 10 \tag{21}$$

where p is the channel index, k is the frequency subcarrier index, and $K = 25$ is the number of PSD samples of each channel. The

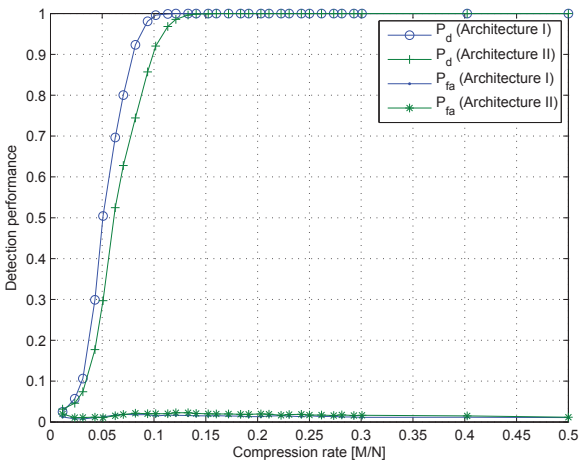

Fig. 5. Detection performance

PSD estimate can be written as

$$\hat{S}_{\mathbf{x},i}(k) = \frac{1}{Q}\sum_{q=1}^{Q}|X_q(k)|^2, \tag{22}$$

where $X_q(k)$ is the Fourier transform of the q-th block of the received time-domain signal $x_q(n)$, n denoting the time sample index, each block containing $2N$ time samples, and $Q = 288$ is the number of blocks. Substituting (22) into (21) we get

$$T_p = \frac{1}{Q}\sum_{k=(p-1)K+1}^{pK}\sum_{q=1}^{Q}|X_q(k)|^2 \tag{23}$$

The decision rule is given by

$$T_p \underset{\mathcal{H}_0}{\overset{\mathcal{H}_1}{\gtrless}} \gamma, \quad p = 1, 2, \ldots, 10 \tag{24}$$

where $\mathcal{H}_1$ and $\mathcal{H}_0$ denote the hypotheses of primary signal being present and absent, respectively, and γ is the decision threshold. Note that under $\mathcal{H}_0$, $T_p/(\sigma_n^2/Q)$ is centralized Chi-square distributed with $2KQ$ degrees of freedom [7]. The false alarm probability P_{fa} can be expressed as

$$P_{fa} = F_r(\frac{\gamma}{\sigma_n^2/Q}) \tag{25}$$

where F_r is the right-tail integral of the χ^2_{2KQ} distribution. The threshold γ is found by fixing P_{fa} to 0.01, i.e., $\gamma = F_r^{-1}(0.01)\sigma_n^2/Q$. The probability of detection P_d is calculated as

$$P_d = \frac{1}{5}\sum_{p=p_1}^{p_5} Pr\{T_p > \gamma\} \tag{26}$$

where $p_i, i = 1, \ldots, 5$ denote the indices of five active channels. Figure 5 shows P_d versus different values of compression rate M/N under a fixed P_{fa} of 0.01. When $M/N < 0.13$, P_d of our approach is a bit worse than that of the method in Section 2.1 due to obtaining a worse estimate of the PSD. When $M/N > 0.13$, P_d under both approaches is close to 1. P_{fa} is around 0.01 as we designed for. Although the MSE performance of our approach is slightly worse compared to the method in Section 2.1 for all compression rates, the detection performances are similar under both approaches for compression rates of interest.

5. CONCLUSIONS

We presented a compressive wide-band spectrum sensing scheme wherein an AIC operates on the received analog signal. Spectrum estimation is done based on CS reconstruction using the autocorrelation vector of the resulting compressed signal. The spectrum estimate was used to determine the spectrum occupancy of the licensed system. Performance evaluation using MSE and probability of detection showed that the proposed scheme performs comparably to the scheme based on [11]. The loss in incoherence thus does not substantially affect spectrum estimation and spectrum occupancy detection.

6. REFERENCES

[1] D. Cabric, I. D. O'Donnell, M. S.-W. Chen and R. W. Brodersen, "Spectrum sharing radios," *IEEE Circuits and Systems Magazine*, pp. 30-45, 2006.

[2] E. Candes, J. Romberg and T. Tao, "Robust uncertainty principles: Exact signal reconstruction from highly incomplete frequency information," *IEEE Trans. on Information Theory*, vol. 52, no.2, pp. 489-509, Feb 2006.

[3] E. Candes and J. Romberg, "Sparsity and Incoherence in Compressive Sampling," *Inverse Problems*, 23(3), pp. 969-985, June 2007.

[4] S. S. Chen, D. L. Donoho, and M. A. Saunders, "Atomic decomposition by basis pursuit," *SIAM Journal on Scientific Computing*,vol. 43, No. 1, pp. 129159, 2001.

[5] D. L. Donoho, "Compressed Sensing," *IEEE Trans. on Information Theory*, vol. 52, no.4, pp. 1289-1306, Apr 2006.

[6] Federal Communications Commission - First Report, and Order and Further Notice of Proposed Rulemaking, "Unlicensed operation in the TV broadcast bands," *FCC 06-156*, Oct. 2006.

[7] S. M. Kay, *Fundamentals of Statistical Signal Processing, Volume 2: Detection Theory*, Prentice Hall, 1998.

[8] S. Kirolos, T. Ragheb, J. Laska, M.F. Duarte, Y. Masssoud, and R. G. Baraniuk, "Practical issues in implementing analog-to-information converters," *IEEE International Workshop on System on Chip for Real Time Applications*, pp. 141-146, Dec 2006.

[9] C. La and M. Do, "Signal reconstruction using sparse tree representations," *SPIE Wavelets XI*, vol. 5914, pp. 59140W.1-59140W.11, Sept 2005.

[10] J. Laska, S. Kirolos, Y. Massoud, R. Baraniuk, A. Gilbert, M. Iwen, and M. Strauss, "Random sampling for analog-to-information conversion of wideband signals," *IEEE Dallas Circuits and Systems Workshop*, pp. 119-122, Oct 2006.

[11] Z. Tian and G. B. Giannakis, "Compressed sensing for wideband cognitive radios," *Proc. of the International Conference on Acoustics, Speech, and Signal Processing*, pp. IV/1357-IV/1360, Apr 2007.

[12] Q. Zhao and B. M. Sadler, "A survey of dynamic spectrum access," *IEEE Signal Processing Magazine*, pp. 79-89, May 2007.